On directed interacting animals and directed percolation

2002 J. Phys. A: Math. Gen. 35 2725

(http://iopscience.iop.org/0305-4470/35/12/303)

INSTITUTE OF PHYSICS PUBLISHING JOURNAL OF PHYSICS A: MATHEMATICAL AND GENERAL

J. Phys. A: Math. Gen. **35** (2002) 2725–2744 PII: S0305-4470(02)31140-5

On directed interacting animals and directed percolation

Milan Knežević[1] **and Jean Vannimenus**[2]

[1] Faculty of Physics, University of Belgrade, PO Box 368, 11000 Belgrade, Yugoslavia
[2] Laboratoire de Physique Statistique de l'ENS[3], 24 rue Lhomond, 75005 Paris, France

E-mail: knez@ff.bg.ac.yu and jean.vannimenus@lps.ens.fr

Received 20 November 2001
Published 15 March 2002
Online at stacks.iop.org/JPhysA/35/2725

Abstract

We study the phase diagram of fully directed lattice animals with nearest-neighbour interactions on the square lattice. This model comprises several interesting ensembles (directed site and bond trees, bond animals, strongly embeddable animals) as special cases and its collapse transition is equivalent to a directed bond percolation threshold. Precise estimates for the animal size exponents in the different phases and for the critical fugacities of these special ensembles are obtained from a phenomenological renormalization group analysis of the correlation lengths for strips of width up to $n = 17$. The crossover region in the vicinity of the collapse transition is analysed in detail and the crossover exponent ϕ is determined directly from the singular part of the free energy. We show using scaling arguments and an exact relation due to Dhar that ϕ is equal to the Fisher exponent σ governing the size distribution of large directed percolation clusters.

PACS numbers: 64.60.Ak, 05.50.+q, 05.70.Jk

1. Introduction

Ever since the seminal work of Broadbent and Hammersley in 1957 [1], the lasting interest in directed percolation and related statistical models has been nurtured by several motivations. Firstly, very anisotropic fractal structures are observed in Nature in a variety of situations where a bias is introduced by an external field or a gradient, ranging from river basins [2] to stress cracks in metals [3] and to lightning discharges. The preferred direction may alternatively correspond to time, with fractal patterns appearing in the dynamics of the systems considered. Pomeau [4] thus proposed that in simple models of turbulence the spatio-temporal structure of the active regions could be described by directed percolation (DP), which was later confirmed

[3] Laboratoire associé au CNRS et aux Universités Paris VI et Paris VII.

by extensive numerical simulations [5–7]. More generally the question arises if the large-scale properties of the observed structures depend on the details of the dynamical processes occurring on short scales, or if they are more universal and can be described in terms of purely statistical models.

Another motivation is that directed systems may be studied using renormalization group (RG) tools, providing a possible approach to non-equilibrium phenomena. The introduction of a preferred direction is a relevant perturbation in the RG sense; it is expected to change the universality class of a phase transition and modify the critical exponents in a non-trivial way. In particular, the DP threshold is in the same universality class as Reggeon field theory [8]. In spite of much work, however, exact results are known only for simpler variants and DP remains a challenge for theorists, being one of the few fundamental problems to remain unsolved in two dimensions—see [9] for a recent review of this model and its position among models of non-equilibrium phase transitions. As pointed out by Grassberger [10], it is surprising in view of the central role played by DP that no detailed experimental tests of the predictions for its critical behaviour have been carried out. A serious difficulty is that in practice many effects can obscure the expected behaviour at attainable scales, so it is of interest to explore the crossover regime between DP and other universality classes.

Directed lattice animals provide another class of fractal structures that may be relevant for oriented systems, and it has been suggested for example that they might describe the large-scale geometry of river networks [11]. The basic animal model consists in enumerating all connected clusters of N sites on a lattice, but various extensions may be considered by introducing local interactions between the cluster sites. In this way one can obtain different statistical ensembles ranging from loopless (lattice trees) to fully compact structures. In contrast with the situation for DP, several exact results are known for directed animals on various lattices [12–16]—for recent results and a review of what is known rigorously see [17] and references therein.

A remarkable connection between the two types of systems has been found by Dhar [18], who showed that a model of interacting directed animals (IDA) can be mapped onto a directed percolation problem if certain relations hold between their respective parameters. For sufficiently strong attractive interactions the typical animals correspond to percolation clusters in the dense phase above the percolation threshold. As a consequence the collapse transition of the IDA model is expected to be of the same nature as the DP threshold, in contrast to the isotropic case where the percolation threshold has been found to correspond to a higher order multi-critical point in the phase diagram of interacting animals [19, 20].

We consider in the present work the statistical properties of fully directed lattice animals with nearest-neighbour interactions on the square lattice, using a transfer matrix approach to calculate their correlation lengths on infinite strips of finite width. The results are analysed using a phenomenological renormalization group method adapted to directed systems [15, 21], which allows an accurate determination of the critical fugacity.

The paper is organized as follows: in the next section the IDA model and the main quantities of interest are introduced and we present the correspondences with a percolation problem and with the generating functions of various simple restricted ensembles. In section 3 we apply the phenomenological renormalization (PR) group approach to non-interacting animals and check its accuracy by comparing the results obtained using strips of widths up to $n = 18$ with the exact values or the best available ones. Section 4 is devoted to the study of the behaviour at the collapse transition temperature; we determine the corresponding critical geometrical and thermal exponents and compare them with DP exponents. The low-temperature regime, which corresponds to the percolating phase of DP, is considered in section 5. In this regime the transition occurring at the critical fugacity is of first order and

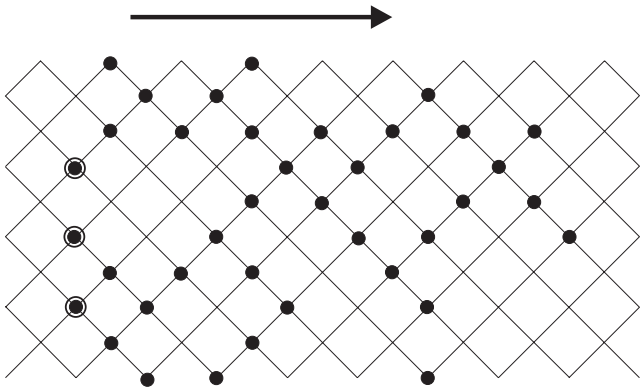

Figure 1. A directed site animal on the square lattice, containing $N = 33$ sites and $P = 37$ pairs of nearest-neighbour sites (filled circles), on a strip of width $n = 4$ with periodic boundary conditions. The root sites are denoted by an extra circle.

the grand partition function displays an essential singularity, but the finite-size PR analysis remains applicable and yields results in excellent agreement with Dhar's prediction for the critical line [18]. In section 6 we obtain very precise values for the critical fugacities of various ensembles, such as bond animals, site or bond trees and strongly embeddable animals [22], and we compare them with published values when these exist. In section 7 particular attention is paid to the crossover region in the immediate vicinity of the collapse transition. Though the singularity is very weak we are able to obtain a direct estimate of the crossover exponent. We present analytic arguments which show that this crossover exponent is equal to the Fisher exponent σ for DP [23], in agreement with our numerical results.

2. The interacting animal model

2.1. Directed animals

A directed animal is a connected cluster of N sites, some of which belong to the root, such that any other site of the animal can be reached from the root by a walk which never goes opposite to the directed axis (see figure 1). In the simplest case, non-interacting animals, one associates the same weight x^N with each cluster having N sites, so the basic generating function is

$$S_0(x) = \sum_N \Omega_N x^N \tag{1}$$

where Ω_N is the number of directed connected clusters having a single site (the origin) as root. The problem of enumerating such objects on lattices was recognized as an interesting combinatorial problem and has received much attention over the last two decades, in part because it turned out to be possible to obtain many exact results concerning the Ω_N, whereas for undirected animals only bounds are known. In particular the generating function (1) is known for the square lattice studied here [14, 17]:

$$S_0(x) = \frac{1}{2}\left(\left(\frac{1+x}{1-3x}\right)^{1/2} - 1\right). \tag{2}$$

For physical applications the metric properties of directed animals are perhaps yet more important. They are best described in terms of two independent characteristic lengths with

asymptotic behaviour of the form

$$R^{\parallel} \sim c_1 N^{\nu^{\parallel}} \qquad R^{\perp} \sim c_2 N^{\nu^{\perp}} \tag{3}$$

where $R^{\parallel}$ provides a measure of the average distance between the root and the most distant sites along the directed axis, while $R^{\perp}$ corresponds to the average distance between two extreme animal sites in the perpendicular (transverse) direction. The value of the perpendicular exponent is known to be $\nu^{\perp} = 1/2$ in $d = 2$, from the exact solution for various lattices [14–16] and in agreement with a field theory argument connecting the large-scale behaviour of directed animals and the dynamics at the Yang–Lee edge singularity [12, 13]. The longitudinal exponent $\nu^{\parallel}$ has proven much more difficult to obtain and is known only numerically [24, 25].

2.2. Branched polymers and interacting animals

Interacting animals are often used as simple lattice models to describe the behaviour of branched polymers in dilute solutions. Indeed, field theory calculations [26] indicate that the existence of loops in animals is irrelevant in the RG sense, so one expects them to belong to the same universality class as branched polymers and to share the same large-scale behaviour. A simple way to take into account the interactions with the solvent is to associate an energy ϵ with every pair of neighbouring occupied sites. This energy corresponds to the difference between the monomer–solvent and the monomer–monomer interaction energies (one can distinguish between chemically bonded pairs and others in mere physical contact [27], but the present simple model already contains much of the physics). At an absolute temperature T the Boltzmann thermal weight associated with each pair is then

$$w = \exp(\epsilon / k_B T) \tag{4}$$

where k_B is the Boltzmann constant. A partition function for polymers made of exactly N monomers may be defined:

$$Z_N(T) = \sum_P \Omega(N, P) w^P \tag{5}$$

where Ω (N, P) is the number of clusters of N sites having P pairs of occupied nearest neighbours (note that all possible polymer topologies contribute to Z_N, this corresponds to a model of 'living polymers' where the monomers may rearrange). At infinite temperature $w = 1$ and one recovers the statistics of an ensemble of equally weighted animals. A good solvent corresponds to $\epsilon \simeq 0$ ($w \simeq 1$), and a poor solvent corresponds to $\epsilon \gg 0$ (large w). The free energy per site in the thermodynamic limit is given by

$$f(T) = \lim_{N \to \infty} -\frac{k_B T}{N} \log Z_N(T). \tag{6}$$

It is often convenient to consider the generating function

$$G(x, w) = \sum_N Z_N(w) x^N = \sum_{NP} \Omega(N, P) x^N w^P \tag{7}$$

which is analogous to a grand partition function and has a singularity for $x = x_c(w)$, the critical fugacity. From (5), (6) and (7) one has

$$f(T) = k_B T \log x_c(w). \tag{8}$$

2.3. Collapse transition and percolation threshold

When the temperature is lowered compact configurations become more probable and the polymers are expected to shrink from an extended state to a dense globular state. In the limit $N \to \infty$ a collapse transition occurs between these two states at a well-defined temperature (for a statistically typical polymer). This transition is described by a critical point, usually referred to as the θ-point, which is analogous to a tricritical point for magnetic systems. It is believed that the average linear size of the polymers at the θ-point scales as N^{ν_θ}, where ν_θ differs from the exponents ν and ν_c corresponding respectively to the extended and dense states. Various lattice models have been proposed for the collapse of isotropic branched polymers [27]. No complete solution of these models on regular lattices is known, and most of them have been studied by numerical methods (see, e.g., [28]) such as Monte Carlo simulation, exact enumeration on lattices, or transfer-matrix calculations coupled with phenomenological renormalization (PR) [29, 30].

For directed animals the corresponding transition was first studied by Monte Carlo simulations [31], within an isotropic scaling approach. Although this assumption did not properly take into account the intrinsically anisotropic nature of directed animals, the value obtained for the θ temperature is found to be in agreement with more accurate approaches.

A central result, due to Dhar [18] and rederived independently in a recent study of the adsorption of interacting animals [32], is the existence of a correspondence between the partition function of directed lattice animals with interactions between first and second neighbours and a site-bond percolation problem on the same directed square lattice. In particular, the IDA first-neighbour model studied here corresponds to a simple bond percolation problem for $w > 2$: a given animal A occurs with probability

$$\mathcal{P}(A) = \frac{1+q}{p}\left(\frac{pq^2}{1+q}\right)^N \left(\frac{1+q}{q}\right)^P \tag{9}$$

and using (5) one obtains the relation

$$\Pr(N) = \sum_{|A|=N} \mathcal{P}(A) = \frac{1+q}{p}\left(\frac{pq^2}{1+q}\right)^N Z_N(w) \tag{10}$$

where the sum bears over all clusters of N sites and

$$p = 1 - q = (w-2)/(w-1) \tag{11}$$

is the associated bond percolation probability. $\Pr(N)$ is the probability that for this value of p a percolation cluster starting from the origin contains precisely N sites. Hence in the thermodynamic limit the free energy per site is given for $w > 2$ by

$$\frac{f(w)}{k_B T} = \log\left(\frac{pq^2}{1+q}\right) - \lim_{N\to\infty} (1/N) \log \Pr(N). \tag{12}$$

For isotropic percolation in d dimensions it has been proved [33] that above the percolation threshold the decay of $\Pr(N)$ is slower than exponential and that there exists a value $p_1 > p_c$ such that for $p > p_1$

$$\log \Pr(N) \sim -CN^{1-1/d} \qquad \text{if} \quad N \to \infty \tag{13}$$

but in fact this behaviour is expected to hold for all $p > p_c$. Physically this just means that most sites of a large finite cluster lie far from its external boundary and belong to its 'bulk', whose effective volume is of the order of the geometric one, while the external boundary that needs to be disconnected from the infinite cluster is not fractal and contains sites of the order of $N^{(d-1)/d}$ [33].

In the directed case large finite percolation clusters are quite rare above p_c and difficult to study directly, but a proof has been outlined recently that in this case also the decay of $\Pr(N)$ is slower than exponential [32] and it is natural to expect that $\log \Pr(N)$ also follows a power-law decay for all $p > p_c$. The second term on the right-hand side of (12) is then negligible in the thermodynamic limit and one obtains a simple equation for the critical line in the low-temperature phase [18]:

$$x_c(w) = \frac{pq^2}{1+q} = \frac{w-2}{w(w-1)^2} \qquad \text{if} \quad w > w(\theta). \tag{14}$$

A remarkable consequence is that the free energy per site is not singular on the low-T side of the transition. The excellent agreement of this relation with our numerical results presented below confirms its validity. As a further consequence the critical temperature of the IDA model studied here is related to the critical probability p_c for the directed bond percolation process on the same lattice:

$$w(\theta) = (2 - p_c)/(1 - p_c). \tag{15}$$

The threshold value p_c as well as the values of DP critical exponents have recently been estimated very accurately using low-density series expansions [34–36], so the thermal critical exponents of collapsing directed animals are also known with high precision. Note, however, that the IDA model is more general than DP as it remains well defined for repulsive interactions ($w < 1$), whereas the equivalence with DP is only valid for $w > 2$. Also, the whole (x, w) plane may be given a physical meaning if the region $x > x_c(w)$ is interpreted as a 'weak gel' stabilized through application of an external pressure [29].

2.4. Special ensembles

Let us remark at this stage that the model defined by (7) contains in its phase diagram several special points related to ensembles defined by simple geometrical properties.

Note firstly that for directed animals the number $\mathcal{L}$ of independent loops is just equal to the number N_2 of sites connected to two occupied predecessors. Every such site contributes two pairs of occupied neighbours in (7) while the other occupied sites contribute only one, except for the origin (for simplicity we consider animals rooted at a single site), so the total number of pairs is $P = 2N_2 + (N - 1 - N_2)$. The number of loops is then

$$\mathcal{L} = P - N + 1 \tag{16}$$

and the loop generating function [17] is given by

$$G_l(y, v) = \sum_{N\mathcal{L}} \Omega(N, \mathcal{L}) y^N v^{\mathcal{L}} \tag{17}$$

$$= vG(y/v, v). \tag{18}$$

In particular one obtains the generating function $G_{st}(y)$ of *site trees* (loopless animals):

$$G_{st}(y) = G_e(y, 0) = \lim_{w\to 0, x\to\infty} wG(x, w) \tag{19}$$

with $y = wx$ fixed.

A simple correspondence exists between non-interacting directed *bond animals* (i.e. clusters of connected directed bonds) and site animals: for every occupied site having only one predecessor consider the bond linking them, while for the N_2 sites with two predecessors consider one of three possibilities, either chosing one of the connecting bonds or keeping both

of them. Since N_2 is equal to the number $\mathcal{L}$ of loops this correspondence implies that the generating function of these bond animals is given by

$$G_b(y) = \sum_{N\mathcal{L}} \Omega(N, \mathcal{L}) y^{N-1-\mathcal{L}} (2y + y^2)^{\mathcal{L}} \tag{20}$$

$$= \frac{1}{y} G_l(y, 2 + y) \tag{21}$$

$$= \frac{1}{x} G\left(x, \frac{2}{1-x}\right) \tag{22}$$

with $x = y/(2 + y)$ and where we have used (17) and (18) to obtain (21) and (22) respectively.

If one now discards from the previous bond configurations all the loop-forming ones (i.e. those with two connecting bonds going to the same site) one is left with directed *bond trees*. The correspondence with site animals just discussed shows that their generating function is given by

$$G_{\mathrm{bt}}(y) = \frac{1}{y} G_l(y, 2) \tag{23}$$

$$= \frac{1}{x} G(x, 2) \tag{24}$$

with $x = y/2$.

Finally, *strongly embeddable* animals [22] correspond to maximally connected bond configurations, in the sense that for a given site animal one systematically keeps the two bonds going to every site with two predecessors (bond trees correspond to minimally connected configurations). Their generating function is then simply

$$G_{\mathrm{emb}}(y) = \sum_{N\mathcal{L}} \Omega(N, \mathcal{L}) y^{N-1-\mathcal{L}} (y^2)^{\mathcal{L}} \tag{25}$$

$$= \frac{1}{y} G_l(y, y) \tag{26}$$

$$= G(1, y). \tag{27}$$

Detailed numerical results for these various ensembles are presented in section 6.

3. Numerical methods and phenomenological renormalization analysis

3.1. Transfer matrix method

Here we shall use the method of transfer matrices coupled to a phenomenological renormalization analysis [37, 38], which was applied to lattice animals in [15, 29]. It is convenient to define the generating function $G_{0\boldsymbol{R}}(x, w)$ for the total number $\omega_{0\boldsymbol{R}}(N, P)$ of directed animals of N sites with P pairs of nearest neighbours connecting the points 0 and $\boldsymbol{R}$:

$$G_{0\boldsymbol{R}}(x, w) = \sum_{NP} \omega_{0\boldsymbol{R}}(N, P) x^N w^P. \tag{28}$$

On a strip of width n with, say, periodic boundary conditions, linear recursion relations may be written between the $\omega_{0\boldsymbol{R}}(N, P)$ for two successive values of the distance R along the strip.

The asymptotic behaviour of $G_{0R}(x, w)$ is dominated by the largest eigenvalue $\lambda_n(x, w)$ of the corresponding transfer matrix $\mathcal{T}_n$:

$$G_{0R}(x, w) \sim [\lambda_n(x, w)]^R = \exp\left(-\frac{R}{\xi_n^{\parallel}(x, w)}\right) \qquad R \to \infty \tag{29}$$

which defines the longitudinal (or parallel) correlation length:

$$\xi_n^{\parallel}(x, w) = -1/\log \lambda_n. \tag{30}$$

This correlation length diverges along the critical line $x = \tilde{x}_n(w)$, where $\tilde{x}_n$ is the smallest positive root of

$$\lambda_n(\tilde{x}_n(w), w) = 1 \tag{31}$$

and the generating function (28) is infinite for $x > \tilde{x}_n(w)$. Let us recall that this line determines the free energy per site of a very large animal of width n, $f_n = k_B T \log \tilde{x}_n(w)$. In a similar way $\lambda_n(x, w)$ determines the average site density $\rho_n(w)$ of an animal on the strip [15, 29] through

$$\rho_n(w) = \frac{1}{n} \frac{\partial \log[\lambda_n(x, w)]}{\partial \log x}\bigg|_{x=\tilde{x}_n} \tag{32}$$

where the derivative is calculated at $\tilde{x}_n(w)$.

The gel phase, for $x > \tilde{x}_n(w)$, will not be studied in the present paper; let us note that expression (32) remains valid and gives the gel density [29], but the expression of the correlation length is different (see [39] for a lucid discussion of that point).

3.2. Phenomenological renormalization in the high-temperature limit

In the high-temperature limit ($w = 1$), one recovers non-interacting lattice animals which as mentioned above have been studied by a variety of methods (see [15, 25, 29] and references cited therein). Let us recall here two recent results. Using the connection of this problem to the continuous-time dynamics of a one-dimensional lattice gas [24], Dhar was able to obtain a very accurate value of the longitudinal size exponent $\nu^{\parallel} = 0.817\,33(5)$, where (5) indicates the estimated uncertainty for the last digit. This critical exponent was estimated more recently [25] by the method of series expansions, which gave $\nu^{\parallel} = 0.817\,22(5)$. Both these results exclude the conjecture $\nu^{\parallel} = 9/11$, which was based on phenomenological renormalization on strips of width up to $n = 12$ [15], and it is now generally believed that $\nu^{\parallel}$ is not a rational number.

We shall first extend the latter calculation on strips of width up to $n = 18$. As we shall show, our estimate of $\nu^{\parallel}$ is in excellent agreement with the results just quoted, which provides a useful check of the overall reliability of the present approach to the case of interacting animals.

According to renormalization-group theory it is expected that for $n \gg 1$ and $x - x_c \ll 1$ the longitudinal correlation length satisfies a finite-size scaling relation of the form

$$\xi_n^{\parallel} \simeq n^{\kappa} F\left[n^{1/\nu^{\perp}}(x - x_c)\right] \tag{33}$$

where the scaling exponent $\kappa = \nu^{\parallel}/\nu^{\perp}$ and the scaling function $F(z)$ is finite and regular for $z = 0$. This allows us to obtain an estimate of the critical fugacity x_c as the fixed point of phenomenological renormalization equations involving three different strips. Using three consecutive widths $(n - 1, n, n + 1)$ the equations for the fixed point read

$$\frac{\xi_{n-1}^{\parallel}(x_{c,n})}{(n-1)^{\kappa_n}} = \frac{\xi_n^{\parallel}(x_{c,n})}{n^{\kappa_n}} = \frac{\xi_{n+1}^{\parallel}(x_{c,n})}{(n+1)^{\kappa_n}} \tag{34}$$

where $x_{c,n}$ and κ_n are respectively estimates of the critical fugacity and the scaling exponent. Eliminating κ_n in (34) gives an equation for $x_{c,n}$:

$$\log \frac{\xi_{n+1}^{\parallel}}{\xi_n^{\parallel}} = \frac{\log \frac{n+1}{n}}{\log \frac{n}{n-1}} \log \frac{\xi_n^{\parallel}}{\xi_{n-1}^{\parallel}} \qquad \text{for} \quad x = x_{c,n} \tag{35}$$

which would yield the exact value of x_c if the scaling relation (33) held rigorously. Finite-size estimates κ_n, $\nu_n^{\perp}$ and $\nu_n^{\parallel}$ of the critical exponents are then obtained from

$$\kappa_n = \frac{\log(\xi_{n+1}^{\parallel}/\xi_n^{\parallel})}{\log[(n+1)/n]} \tag{36}$$

$$\frac{1}{\nu_n^{\perp}} = -\kappa_n + \frac{\log[(\mathrm{d}\xi_{n+1}^{\parallel}/\mathrm{d}x)/(\mathrm{d}\xi_n^{\parallel}/\mathrm{d}x)]}{\log[(n+1)/n]} \tag{37}$$

$$\nu_n^{\parallel} = \kappa_n \nu_n^{\perp} \tag{38}$$

where all ratios and derivatives are evaluated at $x = x_{c,n}$.

To get accurate numerical estimates of the required derivatives we have used here a perturbative expansion method for the transfer matrices as described in [40]. This enabled us to compute the largest eigenvalue derivatives with an accuracy typically better than 10^{-12}. We also took advantage of the fact that the transfer matrix is singular for $w = 1$ (i.e. $\det(\mathcal{T}_n) = 0$) to reduce its size: for instance, for $n = 15$ the matrix size could be reduced from (1223×1223) to (198×198).

3.3. Analysis of the numerical results

In order to extrapolate these finite-size estimates two different extrapolation procedures were used. The first one (to be referred to as extrapolation 1) is based on a simple sequential fit of the form

$$\nu_n^{\perp} = \nu^{\perp} + An^{-\omega_1} + Bn^{-\omega_2} \tag{39}$$

where the estimates of $\nu^{\perp}$ and A, B, ω_1, ω_2 can be obtained from the values of $\nu_n^{\perp}$ for five consecutive widths. One could expect that for large n these estimates take certain limiting values, providing the form (39) is well chosen. It turns out, however, that in some extrapolation procedures considered in this work the effective values of B and ω_2 are rather unstable, which probably indicates that a more complicated form should be used for the next-to-leading correction. In such cases we prefer to keep only the first two terms on the right-hand side of (39), which always seem to lead to a reliable extrapolation. In either case the new sequences of estimates that we calculate are monotonic and they depend on n more weakly than the original ones. The final estimates are obtained by plotting the extrapolated data versus $n^{-\tilde{\omega}}$, where $\tilde{\omega}$ is adjusted to give a smooth convergence.

The second procedure used to extrapolate for $n \to \infty$, which will be referred to here as extrapolation 2, is known as the Bulirsch–Stoer (BST) algorithm [41]. This method includes a free parameter ω which has to be adjusted self-consistently to minimize the fluctuations in the sequences of estimates produced by the BST algorithm. Let us note here that the ranges of ω estimated by this method are in agreement with the corresponding estimates for the leading correction to scaling exponent ω_1 from (39).

Our finite-size estimates together with the extrapolated values for $\nu^{\perp}$, $\nu^{\parallel}$ and x_c are presented in table 1. One can notice the excellent agreement of these extrapolated values with the exact results $\nu^{\perp} = 1/2$, $x_c = 1/3$, while the present result $\nu^{\parallel} = 0.817\,31(5)$ corroborates the best earlier estimates of the longitudinal size exponent.

Table 1. Critical properties of non-interacting directed lattice animals on the strips of a square lattice with periodic boundary conditions. The finite-size estimates are obtained from the renormalization group equations (35)–(38). Extrapolation 1 is based on the three-term fit (39), while extrapolation 2 relies on the BST algorithm. Uncertainties in the last quoted digits are due to the extrapolation procedures and are shown in parentheses.

n	$\nu_n^{\perp}$	$\nu_n^{\parallel}$	$x_{c,n}$
3, 4, 5	0.483 452 612	0.829 035 839	0.333 659 392 915
4, 5, 6	0.489 970 354	0.825 744 198	0.333 462 353 775
5, 6, 7	0.493 175 785	0.823 887 630	0.333 395 848 362
6, 7, 8	0.495 010 984	0.822 687 170	0.333 367 807 660
7, 8, 9	0.496 169 426	0.821 844 121	0.333 354 128 213
8, 9, 10	0.496 951 869	0.821 218 766	0.333 346 732 444
9, 10, 11	0.497 507 400	0.820 736 423	0.333 342 415 719
10, 11, 12	0.497 917 305	0.820 353 299	0.333 339 741 933
11, 12, 13	0.498 229 180	0.820 041 906	0.333 338 005 223
12, 13, 14	0.498 472 489	0.819 784 080	0.333 336 832 461
13, 14, 15	0.498 666 307	0.819 567 315	0.333 336 014 429
14, 15, 16	0.498 823 451	0.819 382 709	0.333 335 427 953
15, 16, 17	0.498 952 800	0.819 223 752	0.333 334 997 468
16, 17, 18	0.499 060 679	0.819 085 572	0.333 334 674 963
Extrapolation 1	0.499 99(3)	0.817 31(5)	0.333 333 33(1)
Extrapolation 2	0.500 00(3)	0.817 30(5)	0.333 333 34(1)
Exact	1/2	—	1/3

4. θ-point behaviour

4.1. Determination of the θ critical temperature

It was shown in [15] that for non-interacting directed animals, the dependence of the average site density (32) on the strip width is of the form

$$\rho_n(w=1) \sim Cn^{\frac{1-\nu^{\parallel}}{\nu^{\perp}}-1} \tag{40}$$

for large n (here and in the following we use C without super- or subscript as generic notation for an undetermined constant). By analogy with this behaviour and with the case of isotropic lattice animals [29] this density is expected to have the following finite-size scaling form in the vicinity of the IDA θ-point:

$$\rho_n(w) \simeq n^{\psi-1} H\left[(w-w(\theta))n^{1/\nu_t^{\perp}}\right] \tag{41}$$

for $n \gg 1$ and $w - w(\theta) \ll 1$, with

$$\psi = (1-\nu_{\theta}^{\parallel})/\nu_{\theta}^{\perp} \tag{42}$$

where $\nu_{\theta}^{\parallel}$ and $\nu_{\theta}^{\perp}$ denote respectively the longitudinal and perpendicular size critical exponents at the θ-point. $H(z)$ is a non-singular scaling function and $\nu_t^{\perp}$, the perpendicular thermal correlation length exponent, is expected to be the same as the perpendicular exponent $\nu_{\mathrm{DP}}^{\perp}$ for directed percolation. Using (32) to calculate ρ_n we have determined the quantities

$$\psi_n(w) = \frac{\log(\rho_n/\rho_{n+1})}{\log[n/(n+1)]} + 1. \tag{43}$$

Due to the scaling form (41) one expects that $\psi_n(w(\theta)) \to \psi$ for $n \gg 1$, so the solutions of the fixed-point equations

$$\psi_{n+1}(w) = \psi_n(w) \tag{44}$$

Table 2. Finite-size estimates of the critical interaction $w(\theta)$ and the geometric exponents at the collapse transition. The estimates $w_n(\theta)$ and $\psi_{\theta,n}$ are obtained from (44), while $\nu^{\perp}_{\theta,n}$ and $\nu^{\parallel}_{\theta,n}$ are computed using equations (35)–(38) for $w = w(\theta) = 3.8145244$. Extrapolation 1 is based on the sequential fit (39) restricted to two terms.

n	$w_n(\theta)$	$\psi_{\theta,n}$	$\nu^{\perp}_{\theta,n}$	$\nu^{\parallel}_{\theta,n}$
4, 5, 6	3.844 929 99	0.765 241 160	0.434 318 716	0.673 635 137
5, 6, 7	3.832 574 14	0.760 117 725	0.432 326 615	0.675 549 201
6, 7, 8	3.826 116 70	0.756 970 160	0.431 222 068	0.676 643 208
7, 8, 9	3.822 421 11	0.754 906 943	0.430 561 122	0.677 317 531
8, 9, 10	3.820 015 45	0.753 483 968	0.430 142 892	0.677 757 109
9, 10, 11	3.818 686 53	0.752 461 914	0.429 866 869	0.678 056 240
10, 11, 12	3.817 693 28	0.751 703 212	0.429 678 725	0.678 266 797
11, 12, 13	3.816 996 62	0.751 124 448	0.429 547 246	0.678 419 088
12, 13, 14	3.816 493 09	0.750 672 740	0.429 453 585	0.678 531 701
13, 14, 15	3.816 119 76	0.750 313 284	0.429 385 894	0.678 616 506
14, 15, 16	3.815 836 85	0.750 022 425	0.429 336 467	0.678 681 344
15, 16, 17	—	—	0.429 301 202	0.678 731 277
Extrapolation1	3.814 53(1)	0.7479(1)	0.4293(1)	0.6789(1)

yield a sequence of estimates $w_n(\theta)$ and $\psi_{\theta,n}$ for the critical weight $w(\theta)$ and the ratio ψ. The results are given in table 2. Note that this two-parameter phenomenological renormalization (PR) group method gives a rather accurate estimate for the Boltzmann critical weight, $w(\theta) = 3.814\,53(1)$. This estimate is even better than that obtained using relation (15) and the result of a one-parameter PR approach for the directed percolation threshold [21]. It is, however, less accurate than the best one: $w(\theta) = 3.814\,524\,4$, deduced from (15) and the value $p_c = 0.644\,700\,185(5)$ recently determined using a one-parameter series expansion method for DP on the square lattice [36]. So, we shall use this last value of $w(\theta)$ in order to estimate $\nu^{\parallel}_{\theta}$ and $\nu^{\perp}_{\theta}$.

4.2. Geometrical critical exponents $\nu^{\parallel}_{\theta}$ and $\nu^{\perp}_{\theta}$

There are different methods to calculate finite-size estimates of two independent critical exponents $\nu^{\parallel}_{\theta}$ and $\nu^{\perp}_{\theta}$. The simplest one is to suppose that the finite-size scaling form (33) holds for each fixed w, which allows one to apply the approach described in the preceding subsection. Thus, using three-strip PR for $w = w(\theta)$ we have obtained two sequences of estimates $\nu^{\parallel}_{\theta,n}$ and $\nu^{\perp}_{\theta,n}$. The results are shown in table 2.

A more sophisticated analysis [29] consists in taking into account explicitly in the scaling function the two independent relevant fields that control the tricritical behaviour near the θ-point. One then writes

$$\xi^{\parallel}_n \simeq n^{\kappa_\theta} F\left[n^{1/\nu_1} u, n^{1/\nu_2} v\right] \tag{45}$$

where to leading order the scaling fields are related to the model parameters by

$$u = a(x - x_\theta) + b(w - w(\theta)) + \cdots \tag{46}$$

$$v = c(x - x_\theta) + d(w - w(\theta)) + \cdots \tag{47}$$

and

$$\kappa_\theta = \nu^{\parallel}_{\theta}/\nu^{\perp}_{\theta}. \tag{48}$$

Table 3. Finite-size estimates for $w = w(\theta) = 3.814\,5244$. The estimates $x_{\theta,n}$ of the critical fugacity are obtained using the PR equation (35), while those of the critical exponents rely on (36) and (53). Extrapolation 1 is based on the sequential fit (39) using only two terms (i.e. three parameters), except for the case of $x_{\theta,n}$, where a five-parameter fit was used. As before, the BST algorithm is used in extrapolation procedure 2.

n	$x_{\theta,n}$	$\nu^{\parallel}_{\theta,n}/\nu^{\perp}_{\theta,n}$	$\nu^{\perp}_{\theta,n}$	$\nu^{\perp}_{t,n}$
6, 7, 8	0.060 0496 104 928	1.569 170 12	0.431 744 944	1.128 564 66
7, 8, 9	0.060 0497 568 952	1.573 118 80	0.430 976 762	1.124 394 01
8, 9, 10	0.060 0498 269 551	1.575 709 08	0.430 445 690	1.121 384 38
9, 10, 11	0.060 0498 630 888	1.577 275 68	0.430 203 390	1.118 543 34
10, 11, 12	0.060 0498 828 566	1.578 540 83	0.429 910 536	1.116 792 17
11, 12, 13	0.060 0498 941 942	1.579 378 27	0.429 743 411	1.115 151 84
12, 13, 14	0.060 0499 009 511	1.579 984 68	0.429 621 850	1.113 771 99
13, 14, 15	0.060 0499 051 063	1.580 431 00	0.429 531 918	1.112 594 17
14, 15, 16	0.060 0499 077 280	1.580 763 71	0.429 464 479	1.111 576 32
15, 16, 17	0.060 0499 094 171	1.581 014 15	0.429 413 361	1.110 687 46
Extrapolation 1	0.060 049 9124(2)	1.5805(5)	0.4294(1)	1.097(1)
Extrapolation 2	0.060 049 9123(2)	1.581(1)	0.4293(2)	1.097(1)

The smaller scaling exponent, ν_1, say, is related to the transverse size of the animals at the θ-point [29], so $\nu_1 = \nu^{\perp}_{\theta}$, while the larger one controls the thermal correlation length, so $\nu_2 = \nu^{\perp}_{t}$.

Now fixing $w = w(\theta)$ one can still use (35) and (36) to obtain a sequence of estimates $x_{\theta,n}$ and $\kappa_{\theta,n}$ for x_θ and κ_θ respectively. The extrapolated values for x_θ (see table 3) are in excellent agreement with the value deduced from (14), $x_\theta = 0.060\,049\,912\,4(10)$. The main uncertainty comes in fact from the value of p_c used to estimate $w(\theta)$.

Taking the partial derivatives with respect to x and w for a given width n (we follow closely the method and notations of [29]), one has at the θ-point

$$\partial_x \xi^{\parallel}_n = n^{\kappa_\theta}\left(a\, n^{1/\nu_1}\,\partial F/\partial u + c\, n^{1/\nu_2}\,\partial F/\partial v\right) \tag{49}$$

$$\partial_w \xi^{\parallel}_n = n^{\kappa_\theta}\left(b\, n^{1/\nu_1}\,\partial F/\partial u + d\, n^{1/\nu_2}\,\partial F/\partial v\right). \tag{50}$$

The unknown constants $a\,\partial F/\partial u$ and $b\,\partial F/\partial u$ may be eliminated using another width m:

$$\frac{\partial_x \xi^{\parallel}_n}{n^{\kappa_\theta+1/\nu_1}} - \frac{\partial_x \xi^{\parallel}_m}{m^{\kappa_\theta+1/\nu_1}} = c\left(n^{1/\nu_2-1/\nu_1} - m^{1/\nu_2-1/\nu_1}\right)\partial F/\partial v \tag{51}$$

$$\frac{\partial_w \xi^{\parallel}_n}{n^{\kappa_\theta+1/\nu_1}} - \frac{\partial_w \xi^{\parallel}_m}{m^{\kappa_\theta+1/\nu_1}} = d\left(n^{1/\nu_2-1/\nu_1} - m^{1/\nu_2-1/\nu_1}\right)\partial F/\partial v. \tag{52}$$

The ratio c/d may in turn be eliminated using a third width l, yielding finally an equation for the exponent $z = \kappa_\theta + 1/\nu_1$:

$$\frac{\partial_x \xi^{\parallel}_n - (n/m)^z\,\partial_x \xi^{\parallel}_n}{\partial_x \xi^{\parallel}_n - (n/l)^z\,\partial_x \xi^{\parallel}_l} = \frac{\partial_w \xi^{\parallel}_n - (n/m)^z\,\partial_w \xi^{\parallel}_m}{\partial_w \xi^{\parallel}_n - (n/l)^z\,\partial_w \xi^{\parallel}_l}. \tag{53}$$

The same calculation may be performed again by exchanging the terms involving ν_1 and ν_2. One finds that $z' = \kappa_\theta + 1/\nu_2$ also satisfies (53), so one expects this equation to have two positive solutions, from which estimates for ν_1 and ν_2 may be obtained since κ_θ has been estimated independently. The numerical results obtained using three consecutive widths are presented in table 3, where it is readily seen that the extrapolated value $\nu^{\perp}_t = 1.097(1)$ agrees with the value of the perpendicular percolation exponent $\nu^{\perp}_{\rm DP} = 1.096\,854(4)$ [36]. The ratio κ_θ is also very close to its directed percolation counterpart $\nu^{\parallel}_{\rm DP}/\nu^{\perp}_{\rm DP} = 1.580\,745(10)$ [36].

This suggests that the correspondence with directed percolation is also valid for the geometric properties of IDA clusters in addition to their thermal critical behaviour. Indeed, one finds that $\nu_\theta^\parallel/\nu_{\rm DP}^\parallel = 0.391\,55(7)$ is very close to the value of the exponent $\sigma = 1/(\beta_{\rm DP}+\gamma_{\rm DP}) = 0.391\,510(2)$ [36]. This is in direct analogy with the relation $\nu_c = \sigma_p \nu_p$ for isotropic percolation, where ν_c is the exponent associated with the typical radius of large clusters [23]. Although interacting animals are related to directed bond percolation clusters through (10) it was not obvious *a priori* that their geometrical exponents should also be related simply to those of DP, as they depend on the behaviour of $G_{\rm OR}(x, w)$ at fixed w and not along Dhar's line.

4.3. Density exponents

Defining now the thermal density exponent β_t through the variation of the density along the critical line:

$$\rho(T) \sim C(w - w(\theta))^{\beta_t} \tag{54}$$

one obtains from the scaling relation (41) and the numerical results above for ψ and $\nu_t^\perp$

$$\beta_t = (1-\psi)\nu_t^\perp = 0.2765(4) \tag{55}$$

in agreement with the percolation exponent $\beta_{\rm DP} = 0.276\,486(8)$ [36].

At a fixed temperature, on the other hand, the density in the gel phase (for $x > x_c(w)$) is expected to vary close to the critical line as [42]

$$\rho(x) \sim C(x - x_c(w))^{\beta_x} \tag{56}$$

where the exponent β_x depends on the temperature and is related through scaling relations to the other critical exponents, yielding

$$\beta_x = \nu_\theta^\parallel + \nu_\theta^\perp - 1 = 0.1082(1) \qquad \text{for} \quad w = w_\theta \tag{57}$$

$$= \nu^\parallel + \nu^\perp - 1 = 0.3173(1) \qquad \text{for} \quad w < w_\theta. \tag{58}$$

We have not checked these predictions numerically.

5. Low-temperature region

5.1. First-order transition and essential singularity

For $w > w(\theta)$ typical animals are in a collapsed state and cover a finite fraction of the lattice sites in the thermodynamic limit. One expects the transition at a fixed temperature to be of first order [29] and the average site density $\rho(x, w)$ to jump from zero to a finite value on the critical line given by $x_c = (w-2)/w(w-1)^2$ in that region.

Using relation (10) the animal generating function may be written as

$$G(x, w) = \sum_N Z_N(w) x^N = \left(\frac{w-2}{w}\right) \sum_N (x/x_c)^N \Pr(N). \tag{59}$$

If we now assume, as discussed in section 2.3, that for all $p > p_c$ the probability of large finite directed percolation clusters varies as

$$\log \Pr(N) \sim -CN^\zeta \tag{60}$$

where $\zeta < 1$, equation (59) is similar to that obtained by Fisher [43] for the droplet model of condensation, with ζ corresponding to a surface energy exponent. He showed that $G(x, w)$ can be expressed as

$$G(x, w) = \int_0^\infty \frac{x}{x_c\,\mathrm{e}^t - x} f(t)\,\mathrm{d}t \tag{61}$$

Table 4. Finite-size estimates of the critical fugacity $\tilde{x}_n(w = 8)$, defined by $\lambda_{\max}(\tilde{x}_n) = 1$, and parallel correlation length on Dhar's line $\xi_n^{\parallel} = -1/\log \lambda_n(x_D)$, with $x_D(w = 8) = 3/196$.

n	$\tilde{x}_n$	$\tilde{x}_n - x_D$	ξ_n
4	0.015 306 166 798 839 312 837	4.43×10^{-8}	$8.881\,453\,6150 \times 10^{4}$
5	0.015 306 125 866 922 874 256	3.42×10^{-9}	$9.219\,906\,1032 \times 10^{5}$
6	0.015 306 122 730 364 804 891	2.81×10^{-10}	$9.332\,798\,5279 \times 10^{6}$
7	0.015 306 122 473 218 244 718	2.42×10^{-11}	$9.286\,632\,4597 \times 10^{7}$
8	0.015 306 122 451 137 529 752	2.16×10^{-12}	$9.127\,164\,6904 \times 10^{8}$
9	0.015 306 122 449 176 587 816	1.97×10^{-13}	$8.887\,199\,9634 \times 10^{9}$
10	0.015 306 122 448 997 933 046	1.83×10^{-14}	$8.590\,864\,2935 \times 10^{10}$
11	0.015 306 122 448 981 326 805	1.73×10^{-15}	$8.256\,206\,4446 \times 10^{11}$
12	0.015 306 122 448 979 758 112	1.66×10^{-16}	$7.896\,881\,5836 \times 10^{12}$
13	0.015 306 122 448 979 607 947	1.61×10^{-17}	$7.523\,289\,9054 \times 10^{13}$
14	0.015 306 122 448 979 593 412	1.58×10^{-18}	$7.143\,373\,9792 \times 10^{14}$
∞	0.015 306 122 448 979 591 837...	0	

where the auxiliary function $f(t)$ vanishes at the origin with an essential singularity of the form $f(t) \sim \exp(-C/t^{\zeta'})$, so $G(x, w)$ as well as all its derivatives remain finite when $x \to x_c$ from below and G has a very weak singularity of the form

$$\log G_{\text{sing}} \sim -\frac{C}{(x_c - x)^{\zeta'}}, \tag{62}$$

with $\zeta' = \zeta/(1 - \zeta)$. In particular, $\zeta' = 1$ if ζ has the same value $1/2$ as for isotropic 2D percolation.

5.2. Numerical results

As discussed in [29, 44] the phenomenological renormalization approach may still be used to determine the critical fugacity, as the parallel correlation length diverges at the transition. A direct application of the three-strip PR approach using (35)–(38) yields results for x_c that converge very rapidly to the value expected from (14). As can be seen from table 4 (see the third column), the finite-size estimates $\tilde{x}_n$ of x_c are already quite good for narrow strips. To obtain such an accurate numerical check of (14) we had to use a mathematical package allowing for high-precision numbers (the precision of our input data was set up to 30 digits).

The exponent κ_n, however, is found to diverge, signalling a failure of (33) to describe adequately the finite-size scaling of $\xi_n^{\parallel}$. A more detailed numerical analysis of the behaviour of $\xi_n^{\parallel}$, for an interaction $w = 8$ deep in the low-T region, shows that it increases exponentially with the width n if one fixes x at the critical value $x_c(w)$ given by (14):

$$\xi_n^{\parallel}(x_c) \sim A \exp(Kn) \tag{63}$$

and that the fugacity $\tilde{x}_n$ at which $\xi_n^{\parallel}$ diverges (i.e. $\lambda_n(\tilde{x}_n) = 1$) converges exponentially towards x_c (see table 4). These results suggest the following finite-size form:

$$\xi_n^{\parallel} \simeq \frac{C}{(\tilde{x}_n - x)^{\lambda}} \simeq \frac{C}{(x_c - x + D\exp(-K'n))^{\lambda}} \tag{64}$$

where $\lambda = K/K'$. Numerically one finds that $K \simeq K' = 2.21(2)$, so we conjecture that $\lambda = 1$.

The average mass of the clusters

$$\langle N(x) \rangle = x\frac{\partial \log G}{\partial x} \tag{65}$$

is dominated by the regular part of $G(x)$ and remains finite when $x \to x_c$ from below at fixed temperature, as well as all the higher moments of the mass distribution, so the mass and linear dimensions of the typical clusters also remain finite. This implies that the characteristic transverse length to be compared with the strip width in a scaling expression remains finite at the transition, which is consistent with the observed divergence of the effective exponent κ_n.

In the zero-temperature limit ($w \to \infty$) the critical fugacity $x_c \to 0$, with $x_c w \to 1$, and the generating function $G(x, w)$ is dominated by the configurations with the largest possible number of pairs of neighbouring occupied sites at fixed N. These correspond to compact animals, having no internal holes and the maximum number of independent loops, or equivalently the minimum number of lateral surface sites (i.e. sites with either the smallest abscissa on a given row or the smallest ordinate on a given column of the underlying square lattice). One would expect these animals to be globular rather than elongated, but it is not clear to us how to extract from the transfer matrix results values for the geometrical exponents of the (extremely rare) large clusters in that regime.

Let us note that the present compact animals are different from the 'directed compact percolation clusters' studied by Essam [45], which just obey the constraint that two diagonally neighbouring sites are necessarily followed by an occupied site. These are themselves a subset of another class of compact clusters studied in the literature, named 'fully directed compact' by physicists [46, 47] and more precisely 'diagonally convex directed' (DCD) by mathematicians [48, 49]. DCD animals may be characterized as having the minimum accessible perimeter for a given length (i.e. unoccupied sites having an occupied predecessor). They have been exactly enumerated with respect to various parameters [48, 50, 51] and are expected to be extremely elongated, with $\nu^{\parallel} = 1$ and $\nu^{\perp} = 0$ (where $\nu^{\perp}$ is associated with the local width at a given large distance from the origin, rather than to the overall animal width [46]).

6. Special points

As pointed out in section 2.4, the phase diagram of interacting directed animals in the (w, x) plane contains several special points related to various ensembles of animals having specific geometric properties.

- Thus from (22) the generating function of bond animals is obtained on the line $w = 2/(1 - x)$. Using strips of width (14, 15, 16) we find this line intersects the critical line $x_c(w)$ for $w_c = 2.285\,08(1)$. This is in agreement with the value $y_b = 0.285\,0875(8)$, obtained for their critical fugacity by Conway *et al* [52] since in the present notation $w_c = 2 + y_b$.
- Bond trees correspond to $w = 2$ according to (24) and we find that the corresponding $x_c = 0.147\,892\,24(1)$, in agreement with (but more precise than) the critical fugacity $y_{bt} = 2x_c = 0.295\,785(10)$ found in [52].
- Site trees correspond to the limit $w \to 0$ with $y = wx$ fixed and finite. They were studied as model B in [15] and their critical fugacity was found there to be $y_{\mathrm{st}} = 0.368\,649(2)$.
- Finally for a site fugacity $x = 1$ one recovers the generating function of strongly embeddable animals, see (27), so their critical fugacity $y_{\mathrm{emb}} = w_c(1)$. We find $y_{\mathrm{emb}} = 0.356\,563\,26(1)$ for this quantity, which does not seem to have been estimated previously in the literature.

A phase diagram summarizing these various results is displayed in figure 2. It is noteworthy that for $w < w_\theta$ the plotted quantity $wx_c(w)$, which according to (18) is just the critical fugacity for animals enumerated accordingly to loop number, varies quasi-linearly

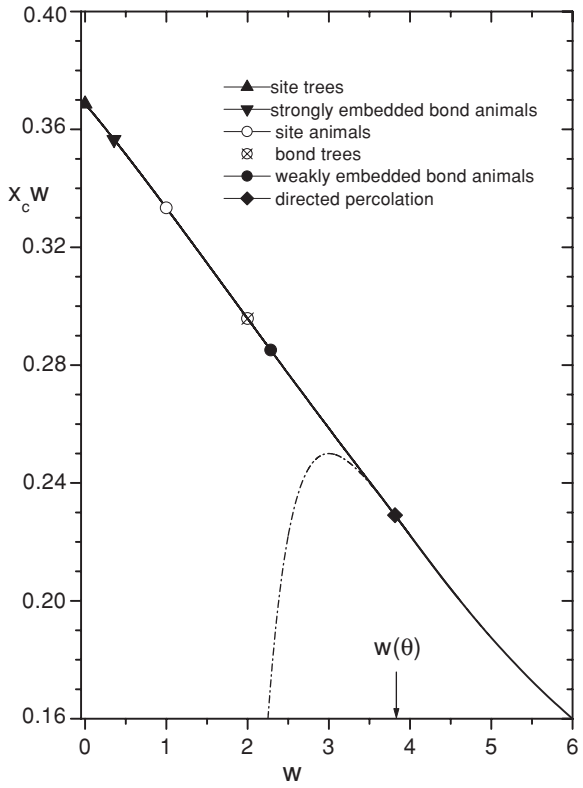

Figure 2. Critical line wx_c versus interaction parameter w. The part of the solid curve for $w > w(\theta)$ corresponds to a first-order transition and is given by (14), the dash-dotted line is its analytic continuation for $w < w(\theta)$. The symbols denote special values of w at which $G(x, w)$ is related to the generating functions of various simple ensembles.

with w, while this is not at all the case for the analytic continuation of the low-temperature expression (14).

7. Crossover region close to the collapse transition

7.1. Critical line and crossover exponent

We now focus our attention on the region close to the θ-point. As noted above, for $w > w(\theta)$ the critical line $x_c(w)$ is given by the simple expression (14) and a remarkable consequence [18] is the absence of a singularity in the bulk free energy per site $f(T)$ when $w \to w(\theta)^+$. The collapse transition is just signalled by a singularity in the size-dependent correction term, which may be interpreted as the vanishing of a surface free energy. For $w < w(\theta)$ the critical line departs from the analytic continuation of (14), which we denote x_D in the following to avoid confusion. The singular part is traditionally written under the form

$$x_c - x_D \simeq C(w(\theta) - w)^{1/\phi} \tag{66}$$

where ϕ is the crossover exponent.

In most cases it is quite difficult to obtain accurate values for such crossover exponents from numerical data, as generally neither the non-singular part of the critical line nor the

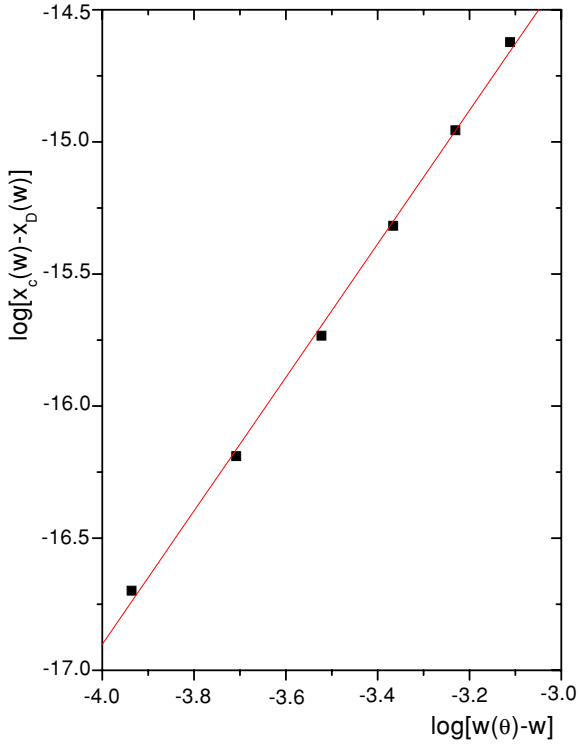

Figure 3. Singular part of the critical fugacity, versus distance to the collapse transition, in a doubly logarithmic plot. The line is a linear fit to the numerical results (filled squares), whose slope yields the value $(\phi)^{-1} = 2.53(5)$ for the crossover exponent.

value of the critical temperature are known with high precision, making a fit of the form (66) subject to large uncertainties. Here the situation is quite favourable as we can take advantage of the analytic nature of the free energy in the low-T phase and of the high-precision knowledge of the critical point $w(\theta)$. The remaining difficulty comes from the uncertainties due to the extrapolation procedure used to obtain $x_c(w)$, which prevent us from analysing reliably the data extremely close to $w(\theta)$. Fortunately there exists an interval of values of w where the extrapolation uncertainties and the corrections to (66) are both small enough to allow a reliable analysis. The numerical results are displayed as a log–log plot in figure 3 and the slope of the curve yields

$$1/\phi = 2.53 \pm 0.05 \tag{67}$$

$$\phi = 0.395 \pm 0.008. \tag{68}$$

This corresponds to a weak singularity for the specific heat measured along the critical line, as the associated exponent α [53] is negative:

$$\alpha = 2 - 1/\phi = -0.53 \pm 0.05 \tag{69}$$

in strong contrast with what is found for the θ-point of isotropic animals, where $\alpha \simeq 0.48$ [29]. This also implies that in the vicinity of their collapse transition interacting directed animals should display geometric properties close to those of critical directed percolation clusters up to large scales.

7.2. Relation with a percolation exponent

In order to derive a relation between the crossover exponent ϕ and a directed percolation exponent, we rewrite (12) under the form

$$\log x_c = \log x_D - \lim_{N\to\infty} (1/N) \log \Pr(N) \tag{70}$$

where $x_D = (w-2)/w(w-1)^2$. For $w < w(\theta)$, the bond probability $p < p_c$ and the cluster probability $\Pr(N)$ is expected to decay exponentially with N, so the second term on the right-hand side of (70) is no longer negligible when $N \to \infty$. Equation (70) may then be written as

$$(1/N)\log \Pr(N) \simeq -\log(x_c/x_D) \qquad \text{for} \quad N \gg 1 \tag{71}$$

$$\simeq -\frac{x_c - x_D}{x_D} \qquad \text{for} \quad x_c - x_D \ll x_D \tag{72}$$

$$\sim C[w(\theta) - w]^{1/\phi} \tag{73}$$

using (66) in the last line. Relation (11) between p and w still holds in the high-T phase, so $w(\theta) - w \simeq (p_c - p)/\left(1 - p_c^2\right)$ and we finally obtain

$$(1/N) \log \Pr(N) \sim C(p_c - p)^{1/\phi}. \tag{74}$$

Now, close to p_c the probability distribution of cluster sizes is expected to follow a scaling law of the form [54]

$$\Pr(N) \sim N^{1-\tau} \Psi\left[N^{\sigma}(p_c - p)\right] \tag{75}$$

for $N \gg 1$ and $z = N^{\sigma}(p_c - p)$ finite, where $\Psi(z)$ is a scaling function finite for $z = 0$ and we have followed the notation of [23] for the Fisher exponents τ and σ. For these two expressions for $\Pr(N)$ to be compatible it is necessary that

$$\phi = \sigma. \tag{76}$$

A very accurate value for σ may be deduced from Jensen's recent results [36] and a standard scaling relation between percolation exponents:

$$\sigma = 1/(\beta_{\mathrm{DP}} + \gamma_{\mathrm{DP}}) = 0.391\,510(2) \tag{77}$$

in good agreement with our numerical value (68) for ϕ, which was obtained without invoking scaling assumptions.

8. Conclusion

We have shown that the combined use of the transfer matrix method and a phenomenological renormalization-group analysis gives very accurate results when applied to interacting directed animals (IDA), in particular, close to their collapse transition. The present results are still not quite as precise for the tricritical fugacity and the tricritical exponents as those obtained from the best series calculations for directed percolation [36], but the method is more flexible; so it could also be applied without excessive effort to situations involving more complicated interactions.

Acknowledgments

We thank M Bousquet-Melou, H Chaté, B Derrida and D Dhar for useful discussions and P Grassberger for providing several relevant references. One of us (MK) would like to thank the University P et M Curie (Paris 6) for financial support and the members of the Laboratoire

de Physique Statistique de l'ENS, where part of this work has been done, for their kind hospitality.

References

[1] Broadbent S R and Hammersley J M 1957 *Proc. Camb. Phil. Soc.* **53** 629
[2] Rodriguez-Iturbe I and Rinaldo A 1997 *Fractal River Basins* (Cambridge: Cambridge University Press)
[3] Herrmann H J 1989 *Physica* D **38** 192
[4] Pomeau Y 1986 *Physica* D **23** 3
[5] Grassberger P and Schreiber T 1991 *Physica* D **50** 177
[6] Rolf J, Bohr T and Jensen M H 1998 *Phys. Rev.* E **57** R2503
[7] Rousseau G 1998 Systémes dynamiques sur réseau *PhD Thesis* ch 3 Université Paris VII webpage http://theses-EN-ligne.in2p3.fr/documents/archives0/00/00/10/79/
[8] Cardy J L and Sugar R L 1980 *J. Phys. A: Math. Gen.* **13** L423
[9] Hinrichsen H 2000 *Adv. Phys.* **49** 815–958
[10] Grassberger P 1997 *Non-Linearities in Complex Systems. Proc. Shimla Conf. on Complex Systems* ed S Puri *et al* (New Delhi: Narosa Publishing) pp 61–89
[11] Green J E and Moore M A 1982 *J. Phys. A: Math. Gen.* **15** L597
[12] Cardy J L 1982 *J. Phys. A: Math. Gen.* **15** L593
[13] Breuer N and Janssen H K 1982 *Z. Phys.* B **48** 347
[14] Dhar D, Phani M K and Barma M 1982 *J. Phys. A: Math. Gen.* **15** L279
[15] Nadal J P, Derrida B and Vannimenus J 1982 *J. Physique* **43** 1561
[16] Dhar D 1983 *Phys. Rev. Lett.* **51** 853
[17] Bousquet-Melou M 1998 *Disc. Math.* **180** 73
[18] Dhar D 1987 *J. Phys. A: Math. Gen.* **20** L847
[19] Coniglio A 1983 *J. Phys. A: Math. Gen.* **16** L187
[20] Janse van Rensburg E J 2000 *J. Phys. A: Math. Gen.* **33** 3653
[21] Kinzel W and Yeomans J M 1981 *J. Phys. A: Math. Gen.* **14** L163
[22] Flesia S, Gaunt D, Soteros C and Whittington S 1993 *J. Phys. A: Math. Gen.* **26** L993
[23] Stauffer D and Aharony A 1992 *Introduction to Percolation Theory* (London: Taylor and Francis)
[24] Dhar D 1988 *J. Phys. A: Math. Gen.* **21** L893
[25] Conway A R and Guttmann A J 1994 *J. Phys. A: Math. Gen.* **27** 7007
[26] Lubensky T C and Isaacson J 1979 *Phys. Rev.* A **20** 2130
[27] Gaunt D S and Flesia S 1990 *Physica* A **168** 602
[28] Whittington S (ed)1998 *Numerical Methods for Polymeric Systems* (Berlin: Springer)
[29] Derrida B and Herrmann H 1983 *J. Physique* **44** 1365
[30] Seno F and Vanderzande C 1994 *J. Phys. A: Math. Gen.* **27** 5813
[31] Lam P M and Duarte J A M S 1987 *J. Stat. Phys.* **49** 245
[32] Janse van Rensburg E J and Rechnitzer A 2001 *J. Stat. Phys.* **25** 49
[33] Kunz H and Souillard B 1978 *J. Stat. Phys.* **19** 77
[34] Jensen I and Guttmann A 1995 *J. Phys. A: Math. Gen.* **28** 4813
[35] Jensen I 1996 *J. Phys. A: Math. Gen.* **29** 7013
[36] Jensen I 1999 *J. Phys. A: Math. Gen.* **32** 5233
[37] Barber M N 1983 *Phase Transitions and Critical Phenomena* vol 8 ed C Domb and J L Lebowitz (London: Academic)
[38] Nightingale M P 1990 *Finite Size Scaling and Numerical Simulations of Statistical Systems* ed V Privman (Singapore: World Scientific)
[39] Foster D P and Seno F 2001 *J. Phys. A: Math. Gen.* **34** 9939
[40] Glaus U 1986 *Phys. Rev.* B **34** 3203
[41] Henkel M and Schütz G 1988 *J. Phys. A: Math. Gen.* **21** 2617
[42] Knežević D, Knežević M and Milošević S 1992 *Phys. Rev.* B **45** 574
[43] Fisher M E 1967 *Physics* **3** 255
[44] Saleur H 1986 *J. Stat. Phys.* **45** 419
[45] Essam J W 1989 *J. Phys. A: Math. Gen.* **22** 4927
[46] Bhat V K, Bhan H L and Singh Y 1988 *J. Phys. A: Math. Gen.* **21** 3405
[47] Privman V and Švrakić N M 1988 *Phys. Rev. Lett.* **60** 1107

[48] Bousquet-Melou M 1996 Combinatoire énumérative *LaBRI Report* 1154-96 webpage http://dept-info.labri.u-bordeaux.fr/bousquet
[49] Feretic S and Svrtan D 1996 *Disc. Math.* **157** 147
[50] Inui N, Katori M, Komatsu G and Kameoka K 1997 *J. Phys. Soc. Japan* **66** 1306
[51] Feretic S 1999 A q-enumeration of directed diagonally convex polyominoes *Proc. 11th FPSAC Conf. (Barcelona)* ed C Martinez, M Noy and O Serra pp 195–206
[52] Conway A R, Brak R and Guttmann A J 1993 *J. Phys. A: Math. Gen.* **26** 3085
[53] Brak R, Owczarek A L and Prellberg T J 1993 *J. Phys. A: Math. Gen.* **26** 4565
[54] Dhar D and Barma M 1981 *J. Phys. C: Solid State Phys.* **14** L1